Supporting Information

Platinum-Based Photothermal Polymer with Intermolecular/Ligand-to-Ligand Charge Transfer for Efficient and Sustainable Solar-Powered Desalination

Miao Zhang[#], Md. Nahian Al Subri Ivan[#], Yingjie Sun, Zikang Li, Shuvra Saha, Safayet Ahmed, Huiying Liu, Yidi Wang, Yuen Hong Tsang* and Wai-Yeung Wong**

1. Experimental Procedures

1.1 Material Synthesis and Characterizations:

All chemicals including raw materials, catalysts and solvents were purchased from Energy Chemical, TCI, Aladdin, Anaqua and Duksan and were used as received unless otherwise specified. ^{1}H NMR and ^{13}C NMR spectra were recorded using a Bruker 400 MHz NMR spectrometer, and chemical shifts were reported as δ values (ppm) with tetramethylsilane (TMS) as the internal reference. Mass spectra were measured by the Bruker Ultraflextreme Matrix Assisted Laser Desorption/Ionization Time-of-Flight (MALDI-TOF) Mass Spectrometer. Fourier-Transform Infrared Spectra (FTIR) were carried out on the FT-IR Spectrometer of Thermo Scientific Nicolet 380. Inductively Coupled Plasma Optical Emission Spectroscopy (ICP-OES) was performed on an Agilent 720 equipment. Thermogravimetric analysis (TGA) was employed based on a Mettler Toledo TGA/DSC 3+ system with a heating rate of 10 °C min^{-1} under a nitrogen atmosphere. UV-Vis-NIR diffuse reflectance spectroscopy (DRS) test was carried out on the Cary 300 UV-Visible Spectrophotometer from Agilent Technologies. Dynamic Light Scattering (DLS) measurement was based on a Zetasizer Advance Range platform.

The ultrafast *fs*-TA measurements were conducted on a *fs* pump-probe system in association with an amplified laser system under ambient conditions, which consist of a mode locked Ti:sapphire seed laser (Spectra Physics, Maitai) directed to a regenerative amplifier (Spitfire Pro, Spectra Physics) and a high power laser (Empower, Spectra Physics) used for pumping and amplifier. The amplified 800 nm output was divided into two parts, and the pump pulses with tuneable wavelength were generated by the major part of the beam (~85%) after an optical parametric amplifier (TOPAS prime, Spectra Physics), while the white-light continuum (WLC) probe and reference pulses (420-780 nm) were generated by the rest part of the beam passing through an optical delay line. A chopper which can modulate the pump pulses was employed to obtain *fs*-TA spectra with and without the pump pulses alternately, and an optics fiber coupled to a multichannel spectrometer with a CMOS sensor was used to record the pump-induced fluctuation in probe/reference beam intensity with adjusting the optical delay line (maximum ~3ns). The spectral profiles were further processed by the Surface Xplorer.

1.2 Solar Evaporator Setup:

The solar evaporation experiments were conducted using a computer controlled electronic balance system (Ohaus Corporation, CP213), beakers of appropriate sizes and a Xenon lamp ((PLS-XSE300, Beijing Perfect light technology co., Ltd) as a solar simulator. Each experiment was conducted for at least 1 hour in an uncontrolled laboratory environment (temperature ≈ 25 ± 2 ºC). The balance system was set to measure and record the mass change data of water every 20 seconds. The light intensity of solar simulator was set to 1 kW m^{-2} (1 sun = 1 kW m^{-2}) using power meter. Before starting each experiment, the intensity of light was measured using power meter (THORLABS, S314C). To measure the temperature of the evaporator and capture the thermal image (IR Image) during evaporation experiment, a thermal camera (FLIR-E64501, Tallinn. Estonia, with an error range of ± 2 °C) was used. The schematic diagram of the OPU-based solar evaporator is depicted in **Figure S4**.

The evaporators had self-floating capability, as shown in **Figure S4**. Therefore, while conducting the experiments the evaporators were placed directly on the top of water. The gap between the evaporator and inner wall of the beaker was filled with a thin polyethylene foam. The thin polyethene foam helped to keep the evaporator stable on one place and facilitate vapor release only through the evaporator. The salinity of natural seawater was measured using EZ-9909SP. A self-made glass box with a sloped glass cover was utilized for collecting the evaporated water.

1.3 Evaporation Rate and Efficiency Calculation:

The **evaporation rate,** m_e**,** can be calculated by the following equation:

$$m_e = \frac{m_h}{A} \tag{1}$$

where, m_h is the hourly mass loss due to evaporation and A is the area of evaporating surface.

The **standard deviation of evaporation rate,** σ**,** of tap water and sea water can be calculated using the following equation:

$$\sigma = \sqrt{\frac{\sum (x_i - \mu)^2}{N}} \tag{2}$$

x_i = each value from the total population

μ = mean of the population

N = number of the population

The **evaporation efficiency,** η_e**,** can be calculated by the following equation[1–5]:

$$\eta_e = \frac{m_{ne}\,(H_{lv} + Q)}{E_i} \tag{3}$$

$$H_{lv} = 1.91846 \times 10^6 \times [T_a/(T_a - 33.91)]^2 \tag{4}$$

$$Q = c * (T_a - T_i) \tag{5}$$

where, m_{ne} is the net evaporation rate (kg m^{-2} h^{-1}),

$m_{ne} = m_e - m_d$ (6)

m_d = dark evaporation rate (kg m^{-2} h^{-1}),

E_i = energy input of the incident light (kJ m^{-2} h^{-1}),

H_{lv}= is the latent heat required for vaporization of water (J kg^{-1}),

T_a = is the average temperature of the solar evaporation surface (K),

Q = is the required heat for increasing the temperature of water,

c = is the specific heat of water (4.2 J g^{-1} K^{-1}),

T_i = initial average temperature of top surface (K)

For 4 mm thick OPU evaporator under 1 sun, $T_a \approx$ 306.4 K, $T_i \approx$ 297 K, $m_e \approx$ 1.57 kg m^{-2} h^{-1}, $m_d \approx$ 0.3 kg m^{-2} h^{-1}, Hence, the η_e of water is about 85.6%. The η_e for sea water is about 83.1% with $m_e \approx$ 1.52 kg m^{-2} h^{-1} and $m_d \approx$ 0.287 kg m^{-2} h^{-1}.

1.4 Heat Loss and Efficiency Calculation according to Gu's method[6]:

Convection loss from OPU surface:

From Newton's law of cooling the **convective heat transfer loss,** q_{conv}**,** can be written as

$$q_{conv} = Ah(T_{as} - T_a) \quad (7)$$

Here,

A = Top surface area of the evaporator

h = Convective heat transfer coefficient of air in natural convection = around 5 W/m^2 K

T_{as} = Average top surface temperature of the evaporator = 33.4 ºC

T_a = Ambient temperature = 25 ºC

The **ratio of the energy loss,** η_{conv}**,** caused by the convective heat transfer can be calculated by the following equation.

$$\eta_{conv} = \frac{q_{conv}}{Aq_s} = \frac{h(T_{as} - T_a)}{q_s} \quad (8)$$

q_s = Incident solar flux per unit area.

The percentage convection heat loss under 1 sun can be calculated as 4.2%.

Thermal radiation loss:

The **energy loss,** q_{rad}**,** due to thermal radiation from the surface of the evaporator can be calculated using Stefan-Boltzmann's equation:

$$q_{rad} = \varepsilon A\sigma(T_{as}^4 - T_a^4) \quad (9)$$

where,

ε = emissivity of the effective surface of the evaporator, and the emissivity of the OPU is considered to be around 0.95.

σ = Stefan-Boltzmann constant = 5.67 X 10^{-8} W/m^2K^4

The **radiation loss rate,** η_{rad}**,** can be calculated by:

$$\eta_{rad} = \frac{q_{rad}}{Aq_s} = \frac{\varepsilon\sigma(T_{as}^4 - T_a^4)}{q_s} \quad (10)$$

The average percentage radiative heat loss under 1 sun can be calculated as 5.003%.

Sensible heat:

The **sensible heat,** q_{sen}**,** can be calculated using the following equation

$$q_{sen} = Cm\Delta T \quad (11)$$

The **percentage sensible heat,** η_{sen}**,** can be calculated as:

$$\eta_{sen} = \frac{q_{sen}}{3600I_0} = \frac{Cm\Delta T}{3600I_0} \quad (12)$$

where C is the specific heat capacity of water (4.2 kJ kg^{-1} K^{-1}), m is the evaporation rate (kg m^{-2} h^{-1}), and ΔT is the temperature difference between the steam and the bulk water. During water evaporation under 1sun the average bulk water temperature was found to be around 28.3 ºC (after 1 hour of evaporation experiment) and average steam temperature was found to be very close to top surface temperature which was 33.6 ºC.

The percentage sensible heat was found to be 1.03%.

From the above three energy transfer channels, the solar-to-thermal and solar-to-steam efficiency can be calculated by the following formulas (Adv. Mater., 2020, 32, 1907975):

$$\eta_{solar\ to\ thermal} = 100\% - 3\% - \eta_{rad} - \eta_{conv} = 87.797\% \quad (13)$$

$$\eta_{solar\ to\ steam} = 100\% - 3\% - \eta_{sen} - \eta_{rad} - \eta_{conv} = 86.767\% \quad (14)$$

The resulting value is very close to the efficiency of 85.6% calculated by our equation.[1-5]

2. Results and Discussion

2.1 PXRD characterization

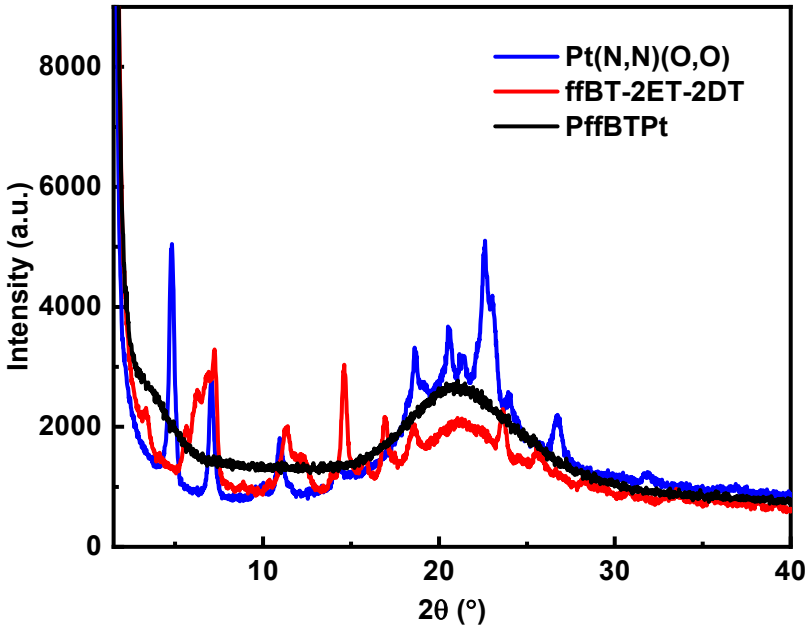

Figure S1. PXRD curves of monomers and polymer in powder state.

2.2 DFT Calculations

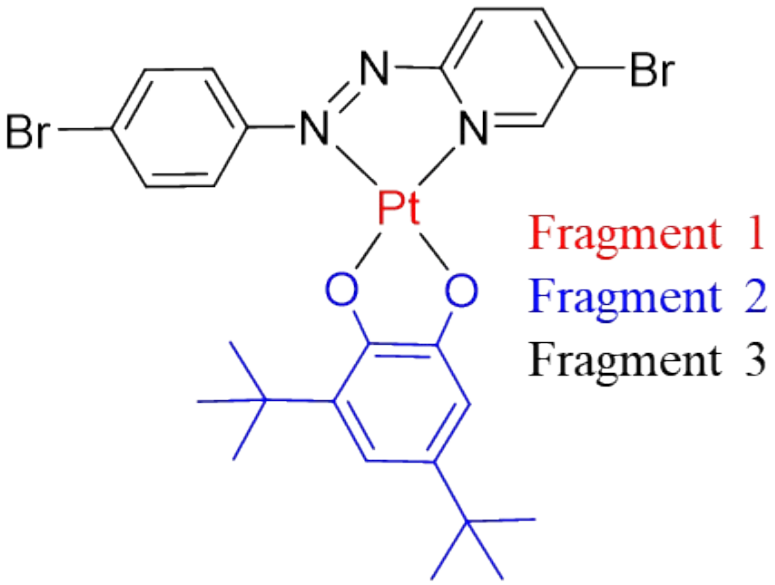

Figure S2. Molecular structure of Pt(N,N)(O,O) and three fragments for IFCT analysis.

Table S1 Summary of IFCT analysis based on the TD-DFT calculations.

Contribution	Hole (%)	Electron (%)	Electron donor	Electron acceptor		
				1	2	3
1	3.2	12.7	1	0.004	0.005	0.022
2	78.4	16.5	2	0.099	0.129	0.555
3	18.4	70.8	3	0.023	0.031	0.131

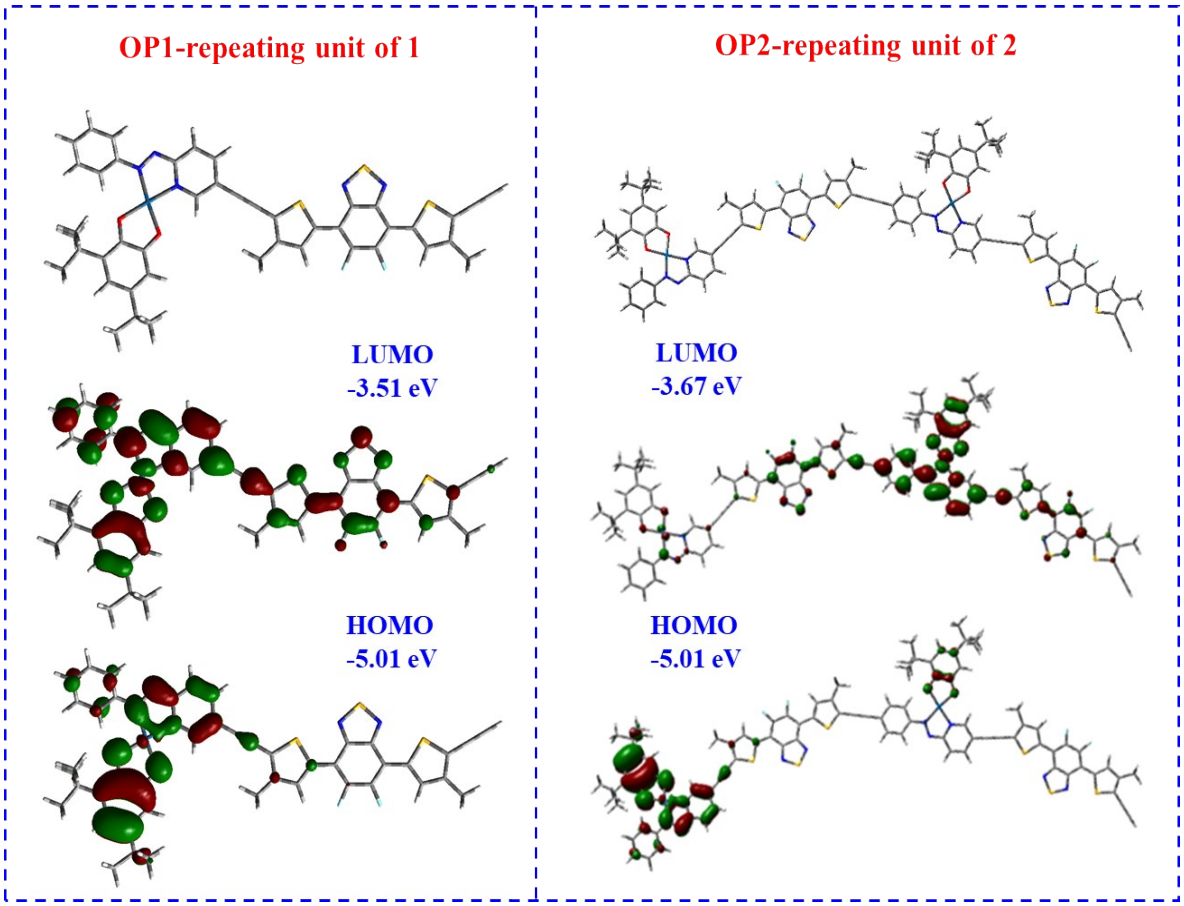
OP1-repeating unit of 1
LUMO
-3.51 eV
HOMO
-5.01 eV
OP2-repeating unit of 2
LUMO
-3.67 eV
HOMO
-5.01 eV

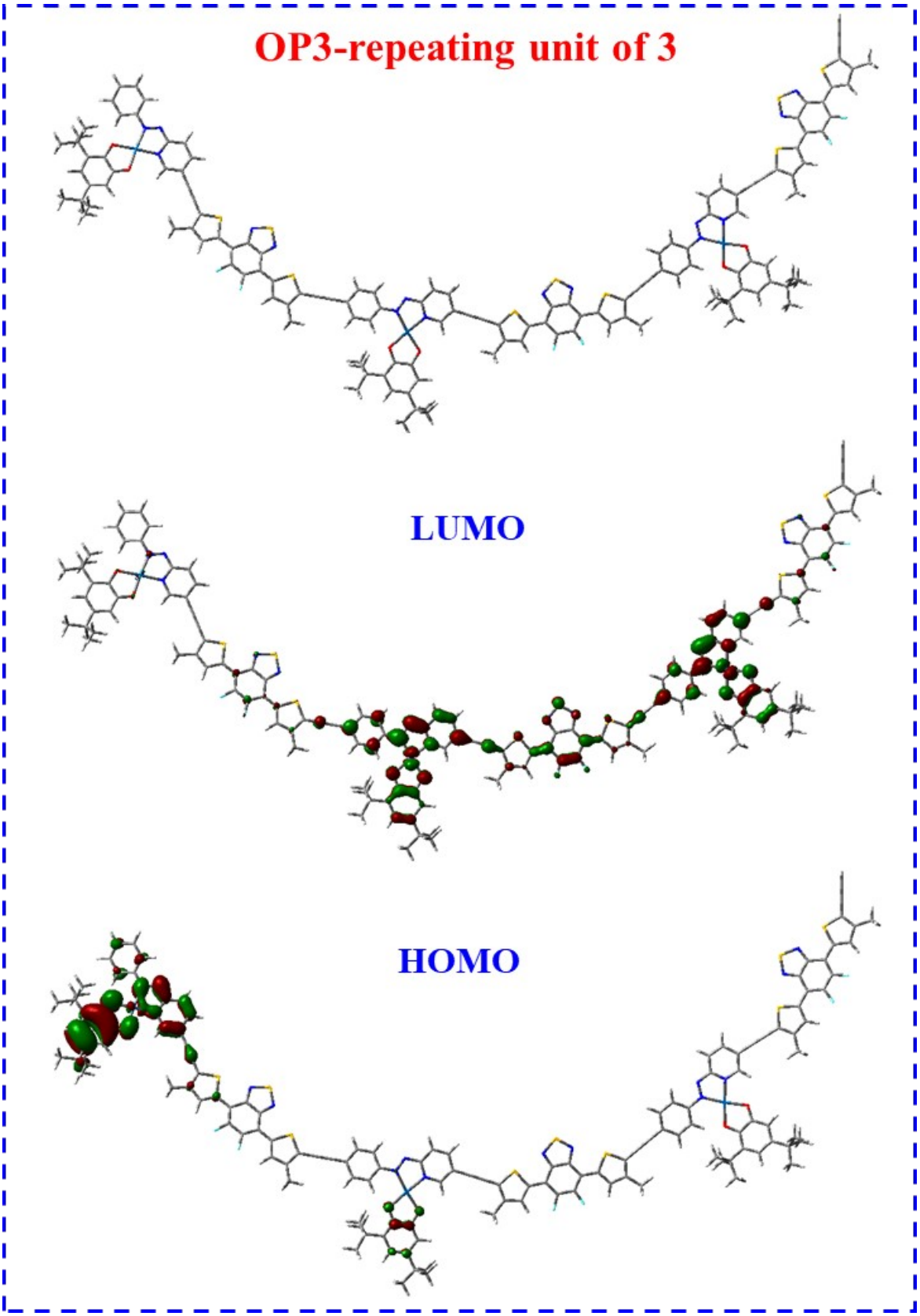

Figure S3. The optimized ground state geometries of OP1, OP2 and OP3 molecules and their LUMO-HOMO electron distribution and the energy states.

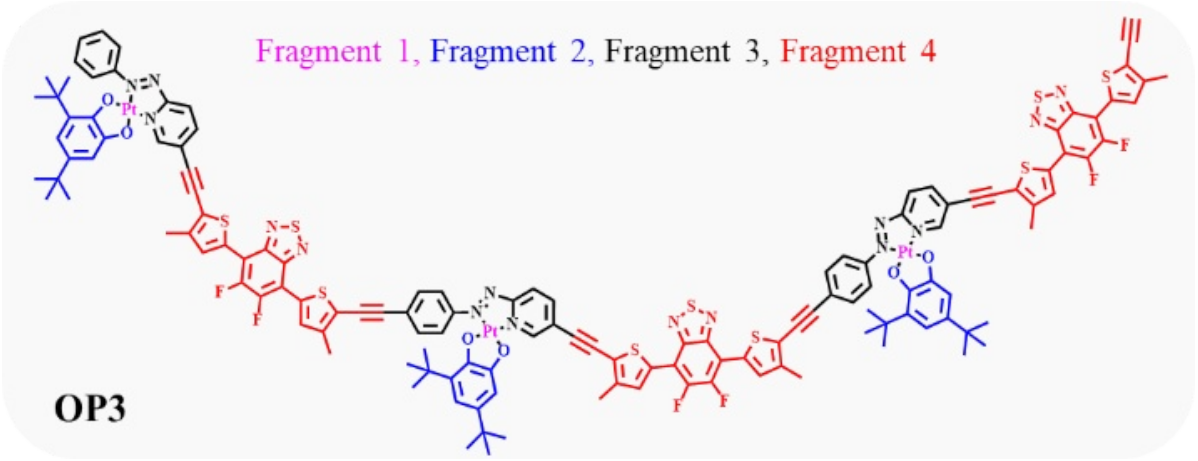

Figure S4. Molecular structure of the OP3 and four fragments for IFCT analysis.

Figure S5. The used solar evaporator system, the self-floating capability of OPU.

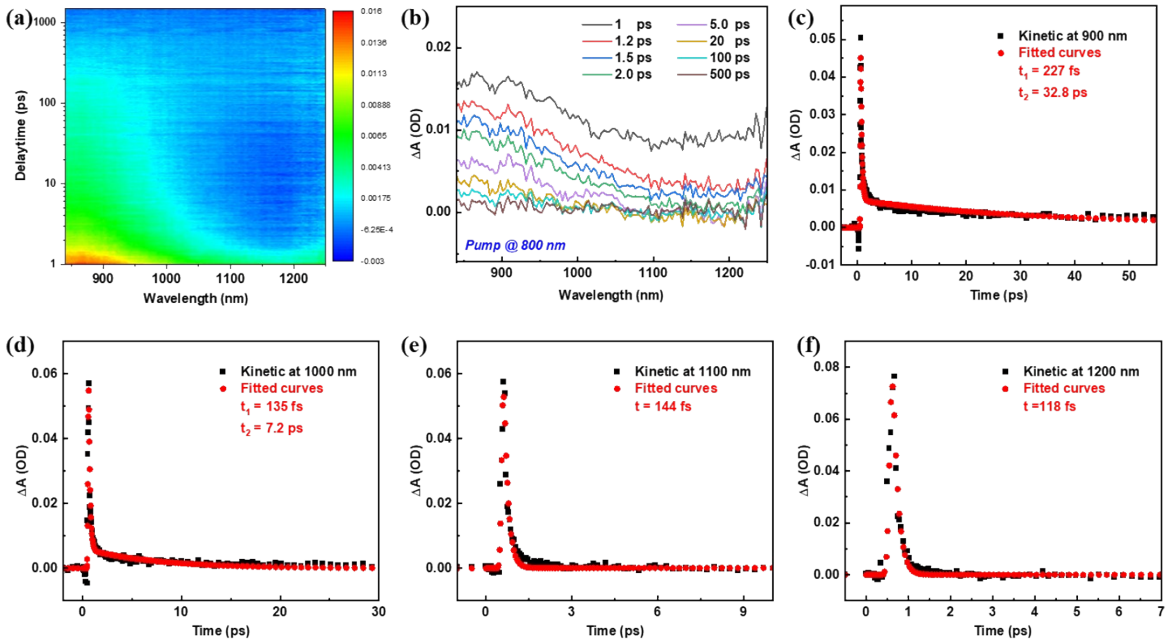

Figure S6. (a) Colour plots of *fs*-TA spectra of PffBTPt. (b) *fs*-TA curves from 830 nm to 1250 nm following excitation with 800 nm laser pulse. (c-f) Corresponding kinetic decay curves and fitting lines at 900 nm, 1000 nm, 1100 nm and 1200 nm.

2.3 Solar Evaporation Performance

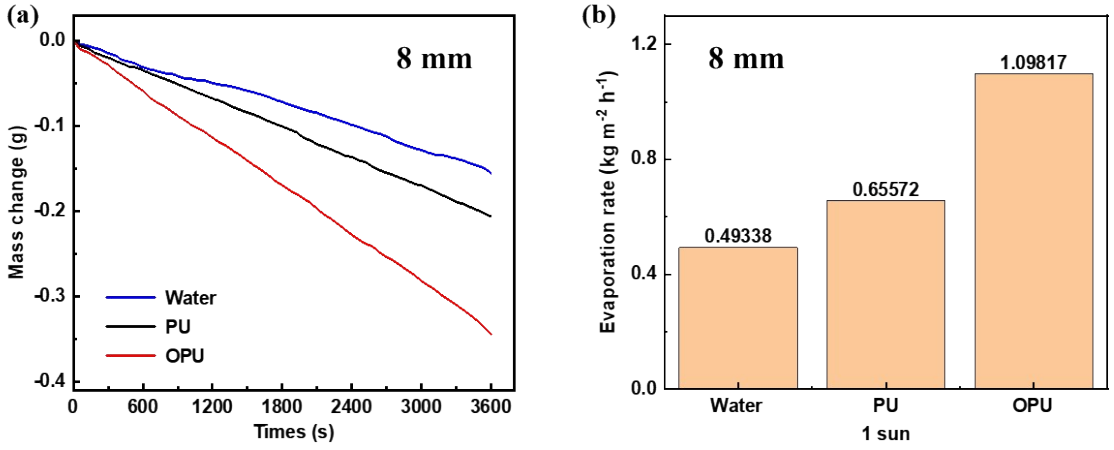

Figure S7. (a) Mass change of evaporator without PU, equipped with 8 nm thick PU and OPU under 1 sun; (b) evaporation rate of the corresponding three samples.

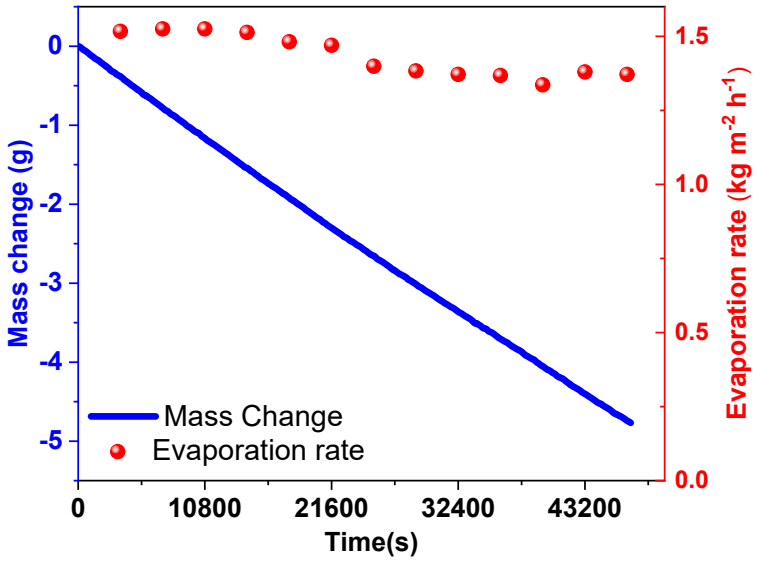

Figure S8. 13 hours long evaporation experiment of natural seawater in the presence of OPU under 1 sun.

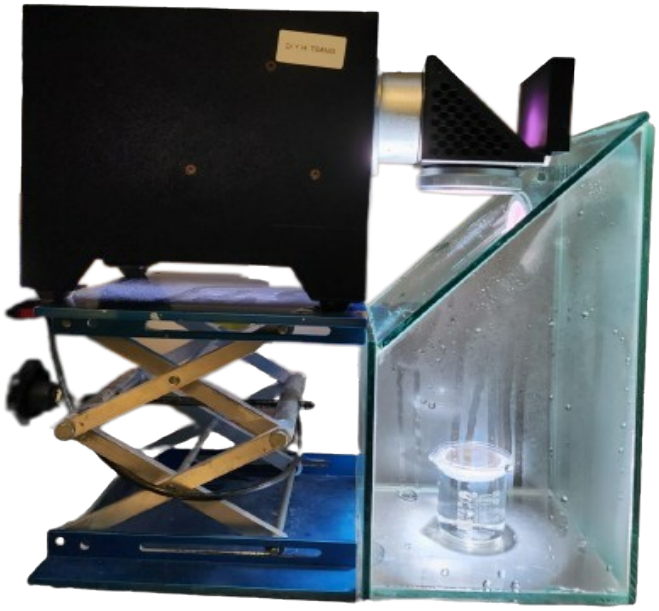

Figure S9. The real picture of the used glass box for collection of the desalinated water.

A glass box is utilized for the collection of purified water. The box is cleaned with IPA followed by DI water and dried carefully inside a drying oven to prevent contamination of the purified water by dust particles. To evaporate a larger quantity of water, a new evaporator with a diameter of 3.7 cm and a thickness of 4 mm was prepared using the same procedure as before. A clean beaker of suitable size is filled with seawater and the large evaporator is placed on the top of the seawater. The gap between the OPU and the inner wall of the beaker is covered by the polyethylene foam to ensure a tight sealing. The outer wall of the beaker is cleaned and

carefully placed inside the glass box to avoid any water spillage. The glass box and Xenon lamp are position on a stable table. As water evaporated, it condenses on the inner wall of glass box and gradually accumulated within it.

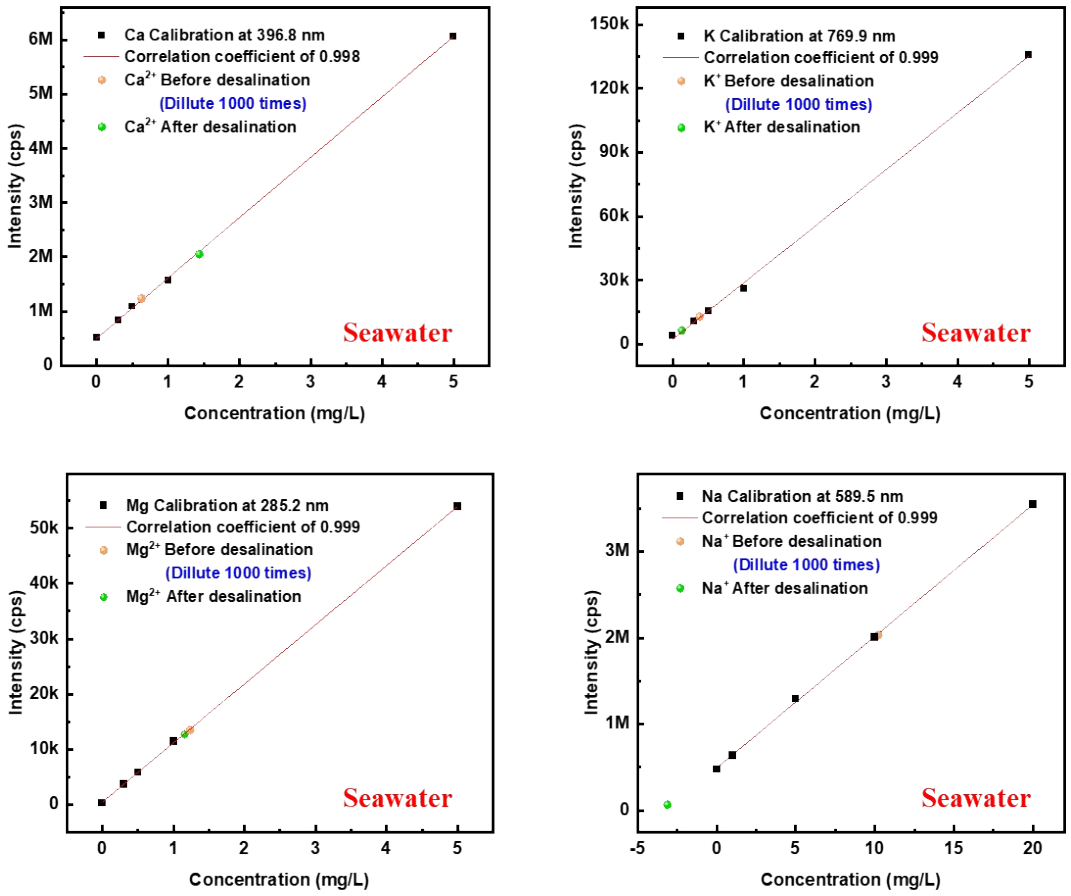

Figure S10. ICP-OES calibration curves of the four cations: Ca^{2+}, K^{+}, Mg^{2+} and Na^{+}.

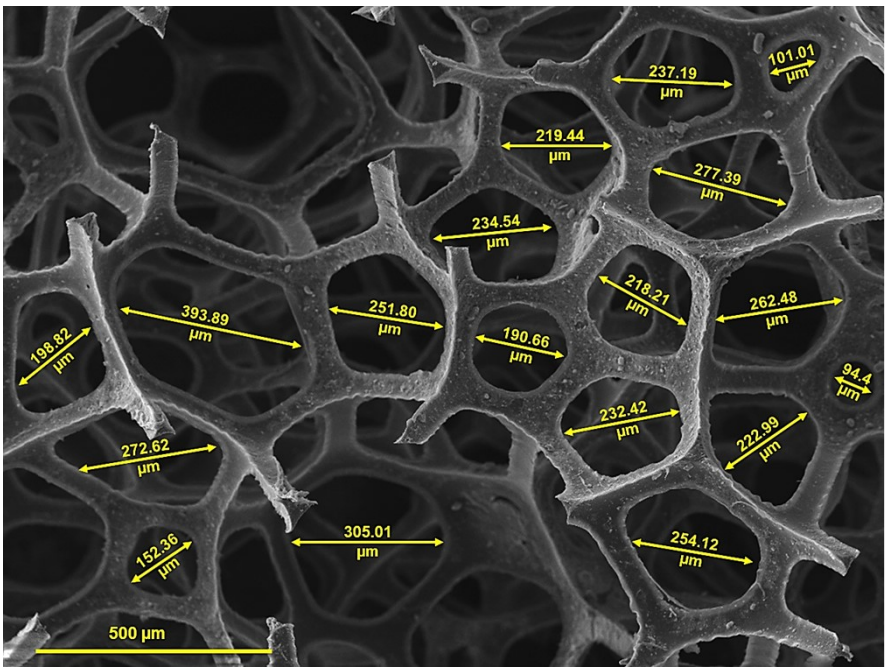

Figure S11. SEM image to show the average diameter of the pores of OPU.

2.4 Synthetic Routes of All Compounds and the Corresponding NMR or MS Spectra

Synthesis of monomer Pt(N,N)(O,O)

Compound 1: 4-Bromoaniline (4.0 g, 1.0 eq.) was dissolved in 100 ml of DCM. The oxone $2KHSO_5 \cdot KHSO_4 \cdot K_2SO_4$ (30 g, 2.0 eq.) was dissolved in 400 ml of water and then added into the DCM solution. The solution was stirred under N_2 at room temperature until TLC monitoring indicated complete consumption of the raw material. Finally, the reaction mixture was washed with the saturated brine water and extracted with DCM, followed by drying over anhydrous Na_2CO_3. The solvent was removed under reduced pressure and the resulting crude product was purified by column chromatography with hexane/DCM as eluent. The compound **1** was obtained as a white solid in 70% yield (3.0 g).

Compound 2: A solution of 5-bromopyridin-2-amine (360 mg, 1.3 eq.) in pyridine (15 ml) was added dropwise into the mixture of aqueous NaOH solution (25%w/w, 5 ml) and compound **1** (300 mg, 1 eq.) in pyridine (10 ml) over 20 min at room temperature. The solution was heated and stirred at 80 °C overnight under N_2 atmosphere and then allowed to cool to room temperature. The reaction mixture was washed with brine, dried with anhydrous Na_2CO_3 and concentrated *in vacuo*. The precipitate was purified by the flash column chromatography with hexane/DCM as the eluent. The compound **2** was obtained as an orange powder in 60% yield (330 mg).

Compound 3: Compound **2** (300 mg, 1.0 eq.) and K_2PtCl_4 (365 mg, 1.0 eq.) in a mixed solvent of acetonitrile/water (18/2 mL) were heated and stirred under a N_2 atmosphere at 120 °C for 24 h. After cooling the mixture to room temperature, the precipitate was collected by filtration and washed with water, and then dried under vacuum without any purification. The product gave a light yellow Pt(II) solid (510 mg) as the compound **3**.

Monomer Pt(N,N)(O,O): The compound **3** (500 mg, 1.0 eq.), 3,5-di-tert-butylcatechol (185 mg, 1.0 eq.) and Na_2CO_3 (440 mg, 5.0 eq.) were dissolved in 1,2-dichloroethane (30 mL) and then the mixture was stirred under a N_2 atmosphere at 80 °C for 24 h. After cooling to room

temperature, the organic solution was removed and the residue was then purified by column chromatography with hexane/DCM as eluent to provide a new product of **Pt(N,N)(O,O)** as the deep green powder in 60% yield (375 mg).

Synthesis of monomer ffBT-2ET-2DT

Compound 4: 11-(Bromomethyl)tricosane (12 g, 1 eq.) was slowly added to a flask of magnesium (1.4 g, 2.0 eq.) and anhydrous THF (100 mL) under a N_2 atmosphere. Crystalline iodine (1-3 mg) was added into the mixture as the initiator to help speed up the reaction. Formation of Grignard was determined by the disappearance of magnesium and a grey solution colour. The completed Grignard was transferred into a dry addition funnel and added dropwise to a stirring mixture of 3-bromothiophene (4.0 g, 0.85 eq.), Ni(II)Cl_2(dppp) (315 mg, 0.02 eq.) and anhydrous THF at 0 ℃ under a N_2 atmosphere. The reaction mixture was allowed to warm to room temperature after addition and refluxed overnight. The reaction mixture was cooled to room temperature and quenched by the diluted HCl, and washed with saturated brine water and extracted with ethyl acetate, then dried over anhydrous Na_2CO_3. The organic layer was concentrated under vacuum. The crude compound was purified by the column chromatography using hexane as the eluent to afford the target compound **4** (9.7 g) with 80% yield as a colourless liquid.

Compound 5: The n-BuLi (2.5 M in hexane, 6 mL, 1.2 eq.) was added dropwise into a solution of compound **4** (5.0 g, 1 eq.) in anhydrous THF (200 mL) at -78 ℃ over 0.5 h under a N_2 atmosphere. The mixture was allowed to warm to room temperature and stirred for another 1 h, then cooled to -78 ℃ again. The trimethyl borate (3 mL, 1.2 eq.) was added dropwise into the cooled reactant followed by 1 h stirring at -78 ℃ and then recovered to room temperature for stirring overnight. After that, the reaction mixture was cooled to room temperature and quenched by the diluted HCl, and washed with saturated brine water, then extracted with ethyl acetate, finally dried over anhydrous Na_2CO_3. The crude product was purified by the flash

column chromatography with hexane/ethyl acetate as the eluent. The compound **5** was obtained as a colourless liquid in 65% yield (4.2 g).

Compound 6: 4,7-Dibromo-5,6-difluoro-2,1,3-benzothiadiazole (1.0 g, 1 eq.), compound **5** (3.7 g, 2.2 eq.), $Pd(PPh_3)_4$ (70 mg, 0.02 eq.) and Cs_2CO_3 (1.0g, 1.1 eq.) were added into anhydrous THF (100 mL) under a N_2 atmosphere. The reaction mixture was vigorously stirred and refluxed at 60 ℃ overnight and then cooled, extracted with DCM. Reaction layer was washed with brine, dried (anhydrous Na_2CO_3) and concentrated *in vacuo*. The residue was collected and purified by the flash column chromatography with hexane/DCM as the eluent. The compound **6** was obtained as a yellow powder in 60% yield (1.8 g).

Compound 7: A solution of NBS (880 mg, 2.5 eq.) in CH_3Cl (30 mL) was added dropwise into the compound **6** (2.0 g, 1 eq.) in CH_3Cl (100 mL) over 15 min in dark condition at room temperature. The reaction mixture was stirred overnight at room temperature, then was washed with brine, extracted with DCM, dried with anhydrous Na_2CO_3 and concentrated in vacuo. The precipitate was purified by the flash column chromatography with hexane/DCM as the eluent to afford compound **7** as a red solid in 70% yield (1.6 g).

Monomer ffBT-2ET-2DT: A mixture of compound **7** (500 mg, 1 eq.), $Pd(PPh3)_2Cl_2$ (30 mg, 0.1 eq.) and CuI (16 mg, 0.2 eq.) were added to anhydrous THF (30 mL) under a N_2 atmosphere. Afterward, the reaction mixture was degassed by a repeated sequence of freeze-pump-thaw cycles for three times. Then, trimethylsilyl acetylene (TMSA) (0.6 mL, 10 eq.) and Et_3N (10 mL) were added to the reaction under a N_2 atmosphere, and the mixture was stirred at 60 °C overnight. After that, the mixture was washed with brine, extracted with DCM, dried with anhydrous Na_2CO_3 and concentrated *in vacuo*. The precipitate was purified by a silica gel column using hexane/DCM as an eluent to give a black compound in 80% yield (415 mg). Then it went through the deprotection step: the prepared black compound (400 mg, 1 eq.) was dissolved in anhydrous THF (20 mL) under a N_2 atmosphere and cooled to -30 ℃. Then the tetra-n-butylammonium fluoride (1 mL, 1.0 M in THF) was added dropwise into the cooled

reactant over 10 min and then stirred for about 1 h. The reaction was quenched with saturated aqueous NH_4Cl and then washed with brine, extracted with DCM, dried with anhydrous Na_2CO_3 and concentrated *in vacuo*. The residue was purified by the column chromatography with hexane/DCM as the eluent to afford monomer **ffBT-2ET-2DT** as a black solid in 70% yield (250 mg).

Synthesis of polymer PffBTPt

Monomer of Pt(N,N)(O,O) (15 mg, 1.0 eq.) and ffBT-2ET-2DT (21 mg, 0.98 eq.), $Pd(PPh_3)_4$ (5.0 mg, 0.2 eq.) and CuI (2 mg, 0.5 eq) were dissolved into 10 mL of 1,4-dioxane with an addition of 2 mL of Et_3N under a N_2 atmosphere. Then the mixture was degassed via the freeze pumping three times to remove oxygen residue followed by heating and stirring in room temperature for 12 h. The precipitate was collected by filtration and washed with water, and further purified by the Soxhlet extraction with methanol, acetone and hexane in turn for 12 h, respectively. The polymer of **PffBTPt** was collected and dried under vacuum for 24 h as a black powder with 93% yield (30 mg). The structure of the polymer was confirmed through FTIR spectra and ICP-OES characterization.

2.4.1 ^{1}H NMR spectra of intermediates of Pt(N,N)(O,O).

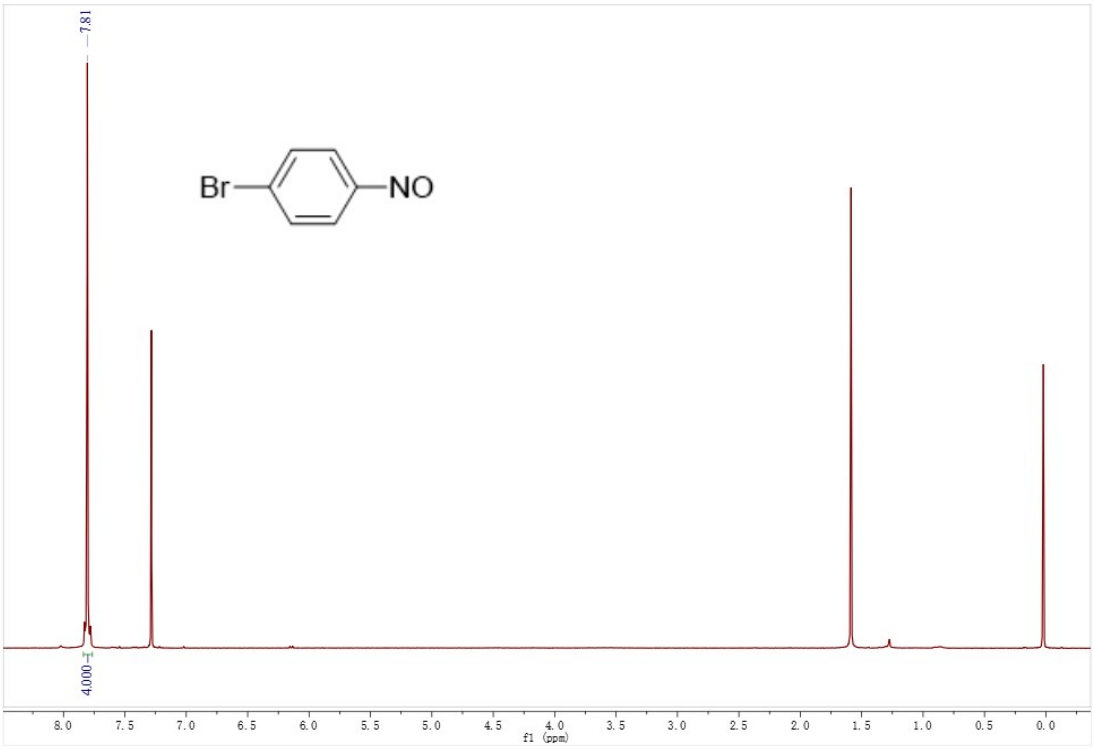

^{1}H NMR (400 MHz, Chloroform-*d*) of **Compound 1**: δ 7.81 (m, *J* = 1.3 Hz, 4H).

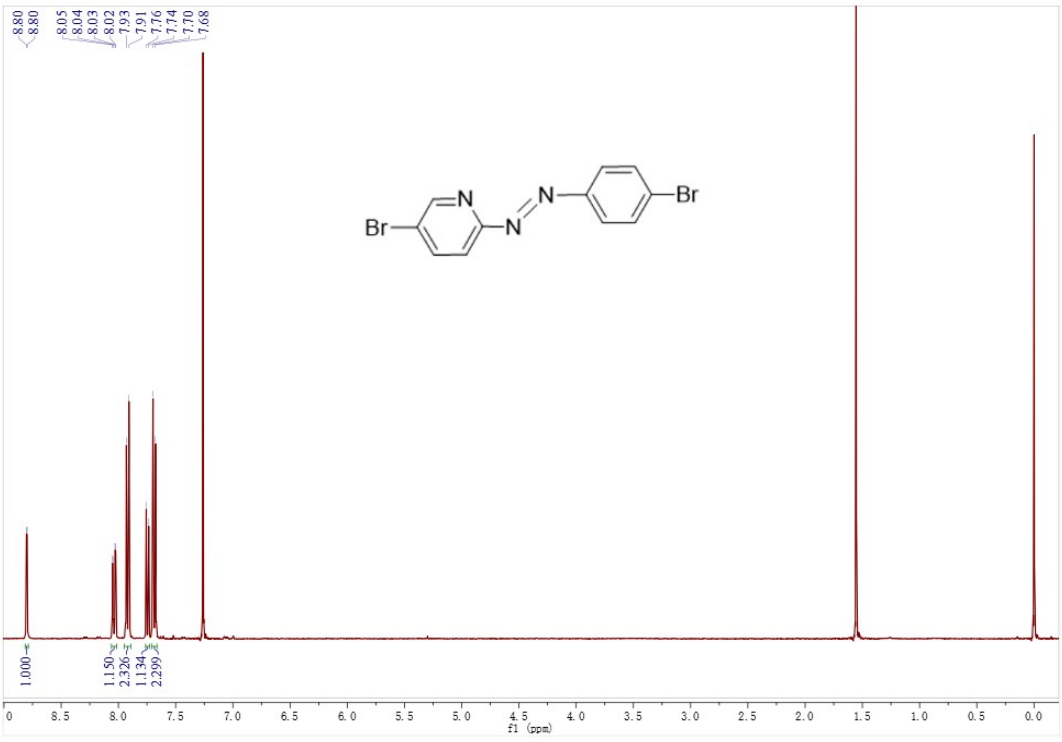

^{1}H NMR (400 MHz, Chloroform-*d*) of **Compound 2**: δ 8.80 (d, *J* = 2.4 Hz, 1H), 8.04 (dd, *J* = 8.5, 2.4 Hz, 1H), 7.92 (d, *J* = 8.7 Hz, 2H), 7.75 (d, *J* = 8.5 Hz, 1H), 7.69 (d, *J* = 8.7 Hz, 2H).

2.4.2 ^{1}H NMR, ^{13}C NMR and MS spectra of complex monomer of Pt(N,N)(O,O).

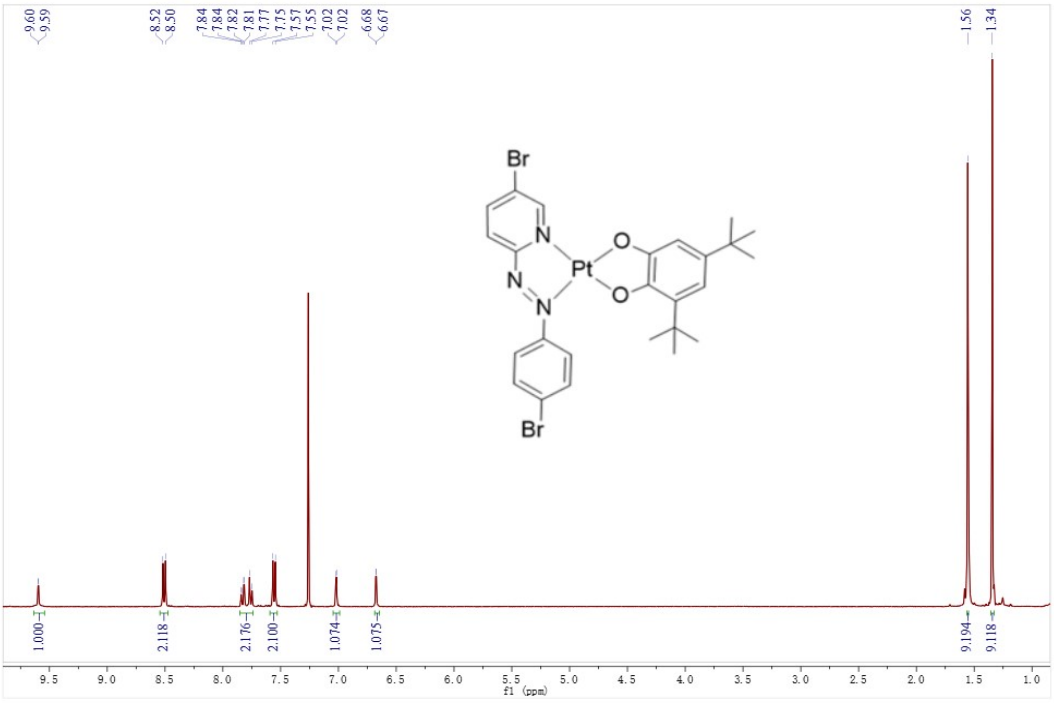

^{1}H NMR (400 MHz, Chloroform-*d*) of **monomer Pt(N,N)(O,O)**: δ 9.59 (d, *J* = 1.9 Hz, 1H), 8.50 (d, *J* = 8.7 Hz, 2H), 7.84 – 7.71 (m, 2H), 7.55 (d, *J* = 8.6 Hz, 2H), 7.01 (s, 1H), 6.67 (d, *J* = 2.2 Hz, 1H), 1.55 (s, 9H), 1.34 (s, 9H).

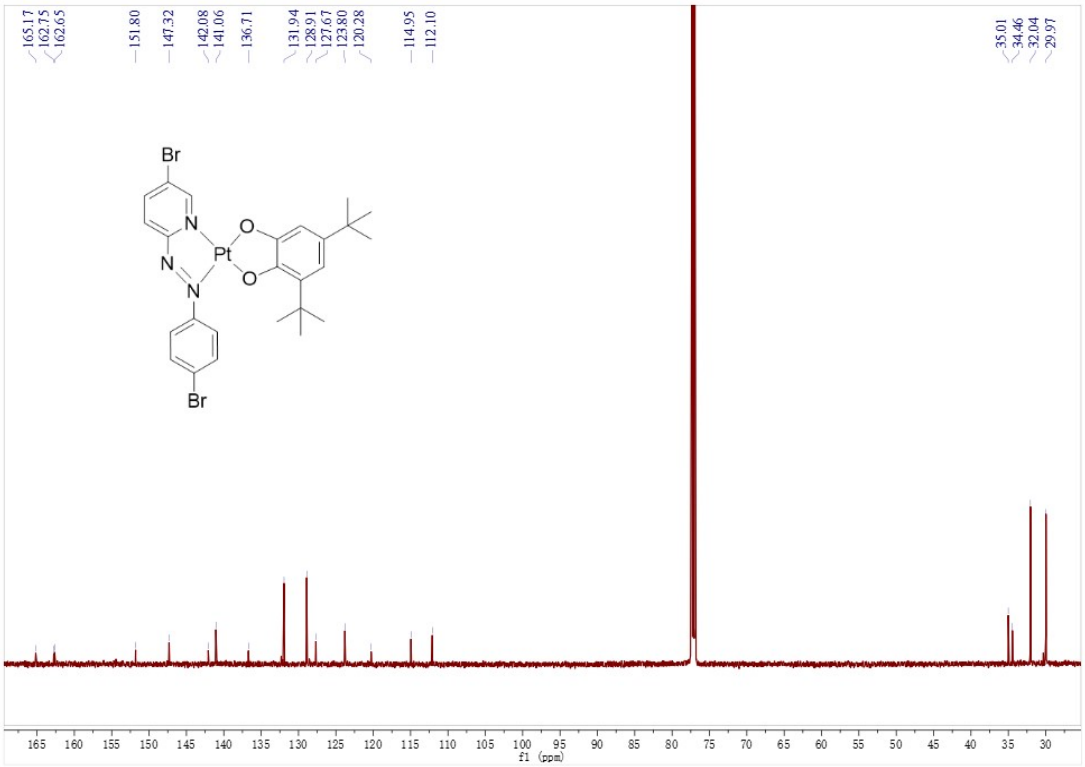

^{13}C NMR (151 MHz, Chloroform-*d*) of **monomer Pt(N,N)(O,O)**: δ 165.17, 162.75, 162.65, 151.80, 142.08, 141.06, 136.71, 131.94, 128.91, 127.67, 123.80, 120.28, 114.95, 112.10, 35.01, 34.46, 32.04, 29.97.

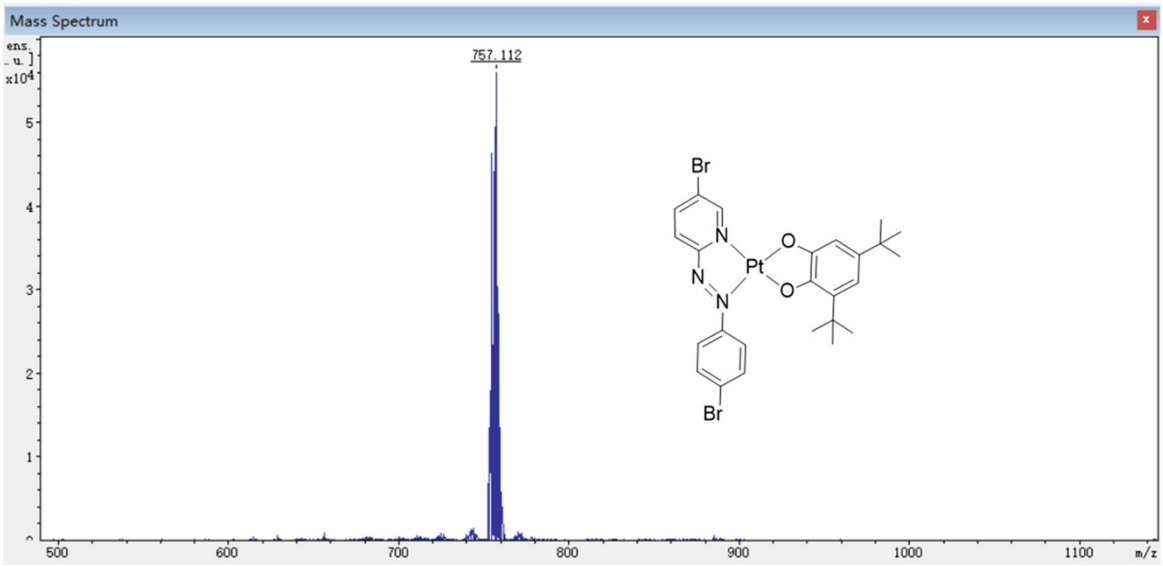

MALDI-ToF MS m/z: $[M+H]^+$ calcd. for $C_{25}H_{27}Br_2N_3O_2Pt$, 756.01; found, 757.112.

2.4.3 ^{1}H NMR spectra of intermediates of ffBT-2ET-2DT.

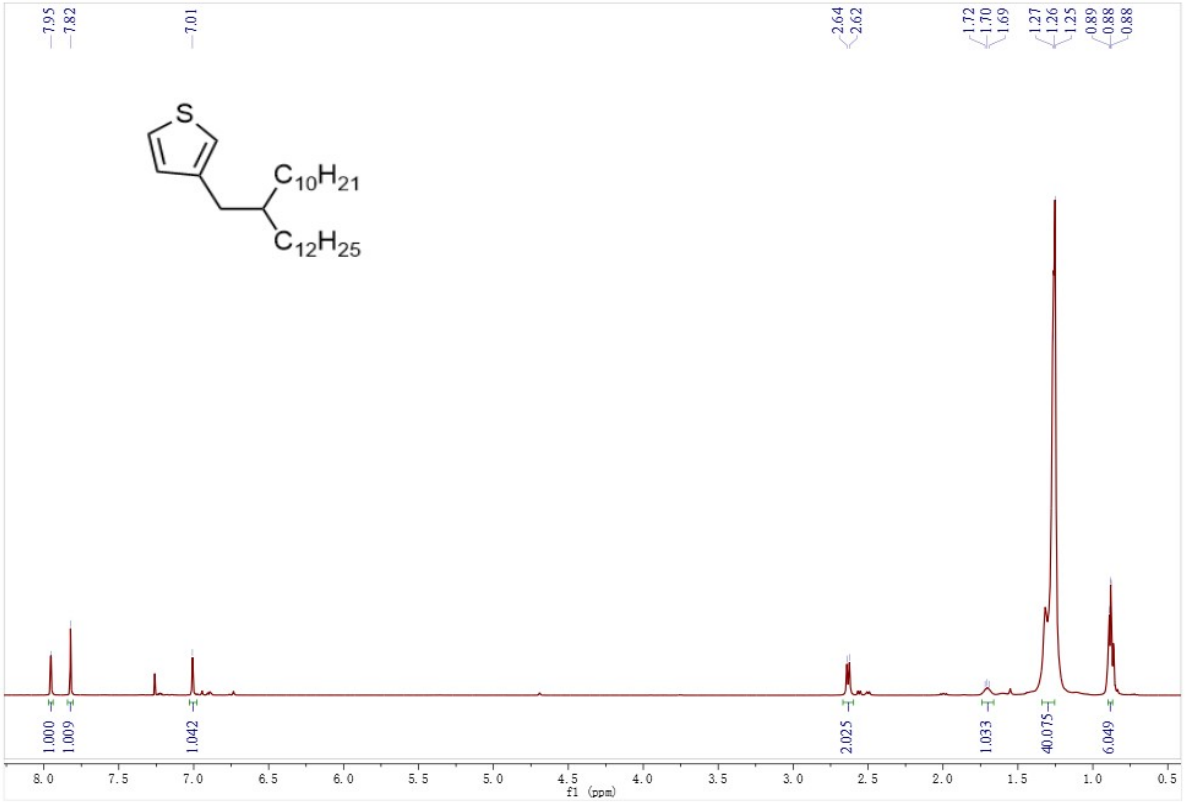

^{1}H NMR (400 MHz, Chloroform-*d*) of **Compound 4**: δ 7.95 (s, 1H), 7.82 (s, 1H), 7.01 (s, 1H), 2.63 (d, *J* = 6.8 Hz, 2H), 1.70 (t, *J* = 5.9 Hz, 1H), 1.26 (d, *J* = 3.1 Hz, 40H), 0.90 – 0.87 (m, 6H).

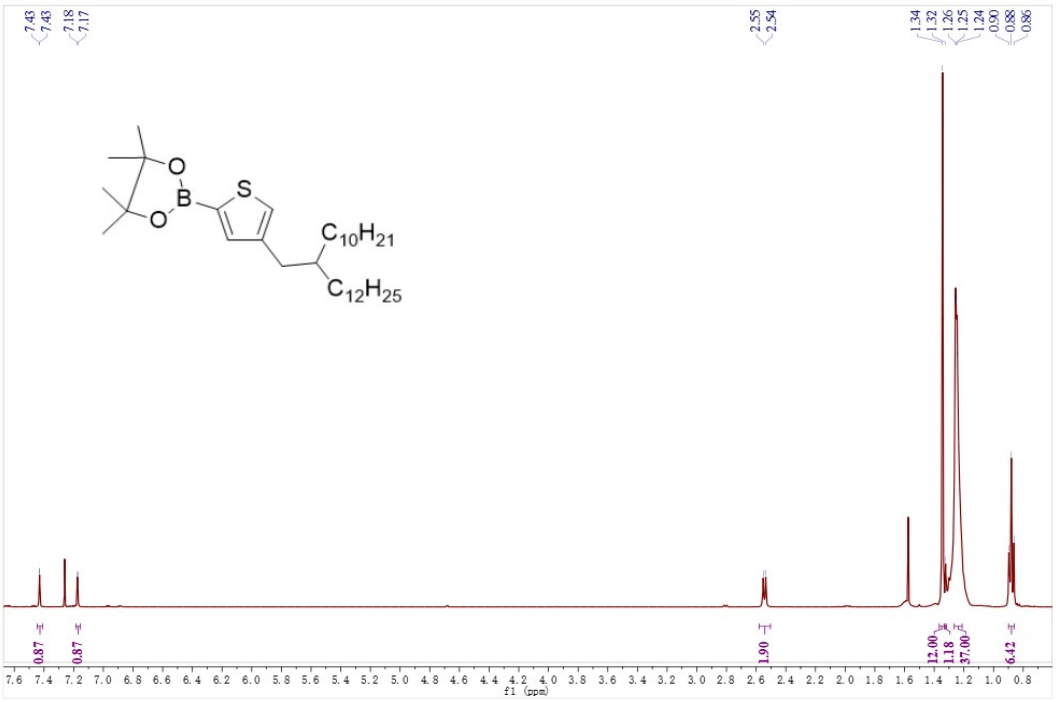

^{1}H NMR (400 MHz, Chloroform-*d*) of **Compound 5**: δ 7.43 (d, *J* = 1.2 Hz, 1H), 7.17 (d, *J* = 1.2 Hz, 1H), 2.55 (d, *J* = 6.8 Hz, 2H), 1.61 (dd, *J* = 8.2, 4.1 Hz, 1H), 1.34 (s, 12H), 1.25 (d, *J* = 4.9 Hz, 40H), 0.88 (t, *J* = 6.8 Hz, 6H).

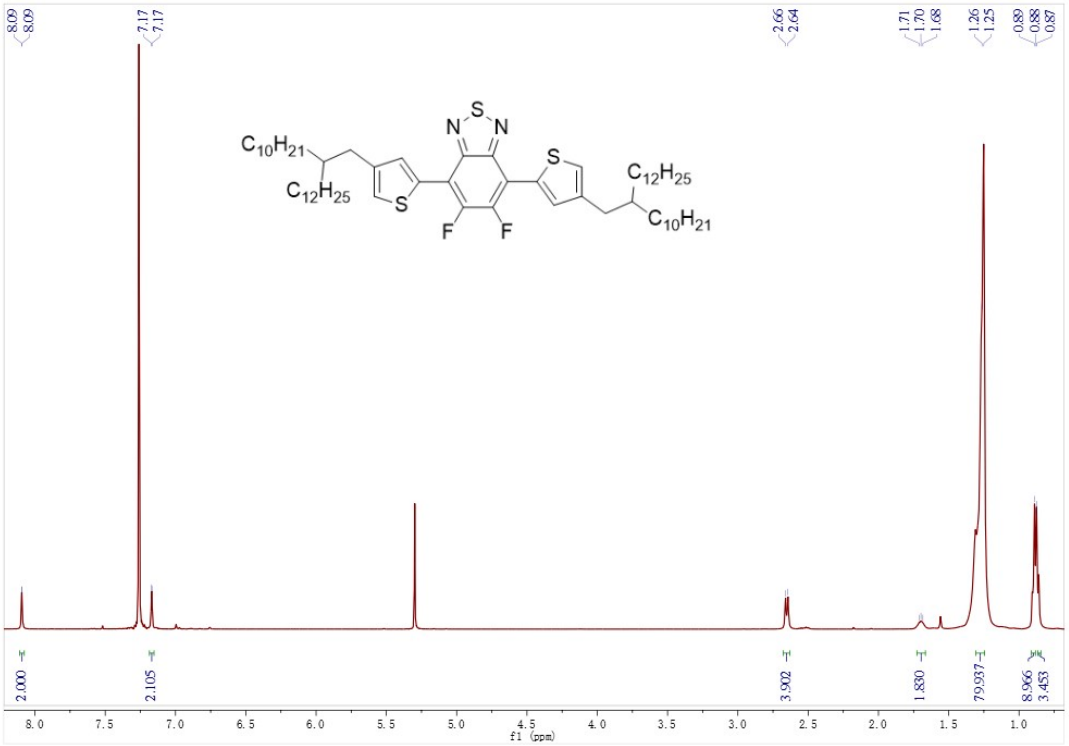

^{1}H NMR (400 MHz, Chloroform-*d*) of **Compound 6**: δ 7.95 (d, *J* = 1.4 Hz, 2H), 7.82 (s, 2H), 7.01 (d, *J* = 1.3 Hz, 2H), 2.63 (d, *J* = 6.7 Hz, 4H), 1.71 (q, *J* = 6.0 Hz, 2H), 1.35 – 1.22 (m, 80H), 0.88 (td, *J* = 6.9, 1.8 Hz, 12H).

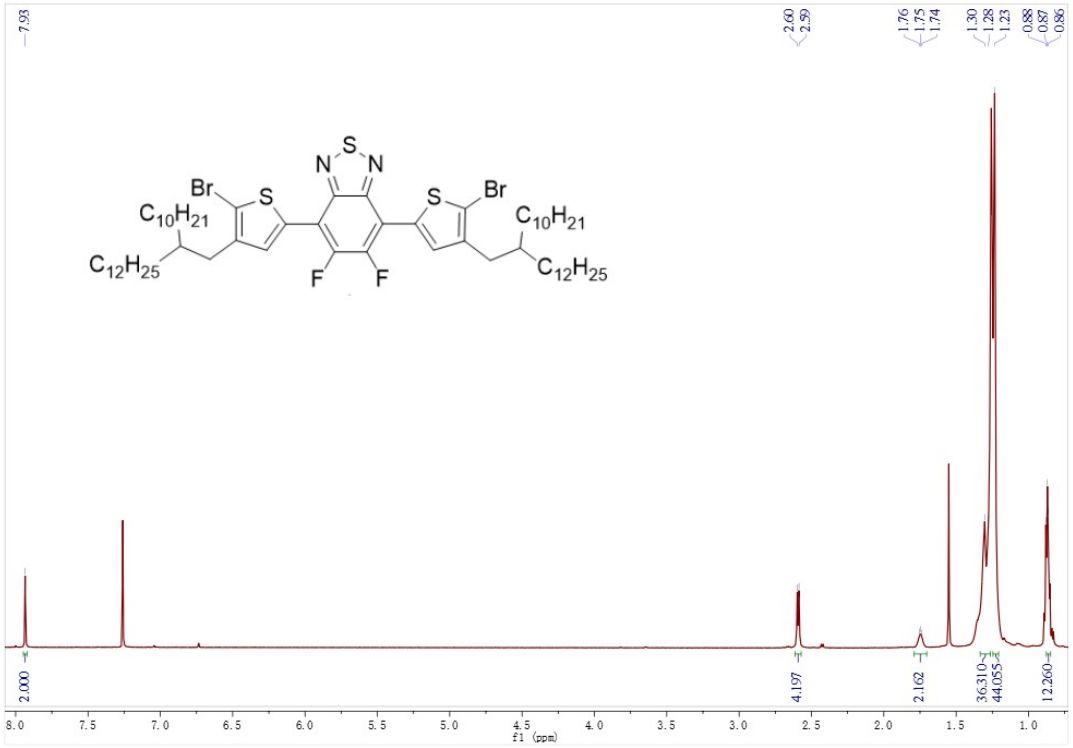

^{1}H NMR (400 MHz, Chloroform-*d*) of **Compound 7**: δ 7.75 (d, *J* = 3.3 Hz, 4H), 2.57 (d, *J* = 7.1 Hz, 4H), 1.75 (s, 2H), 1.34 – 1.21 (m, 80H), 0.87 (td, *J* = 6.9, 2.8 Hz, 12H).

2.4.4 ^{1}H NMR spectra of organic monomer of ffBT-2ET-2DT.

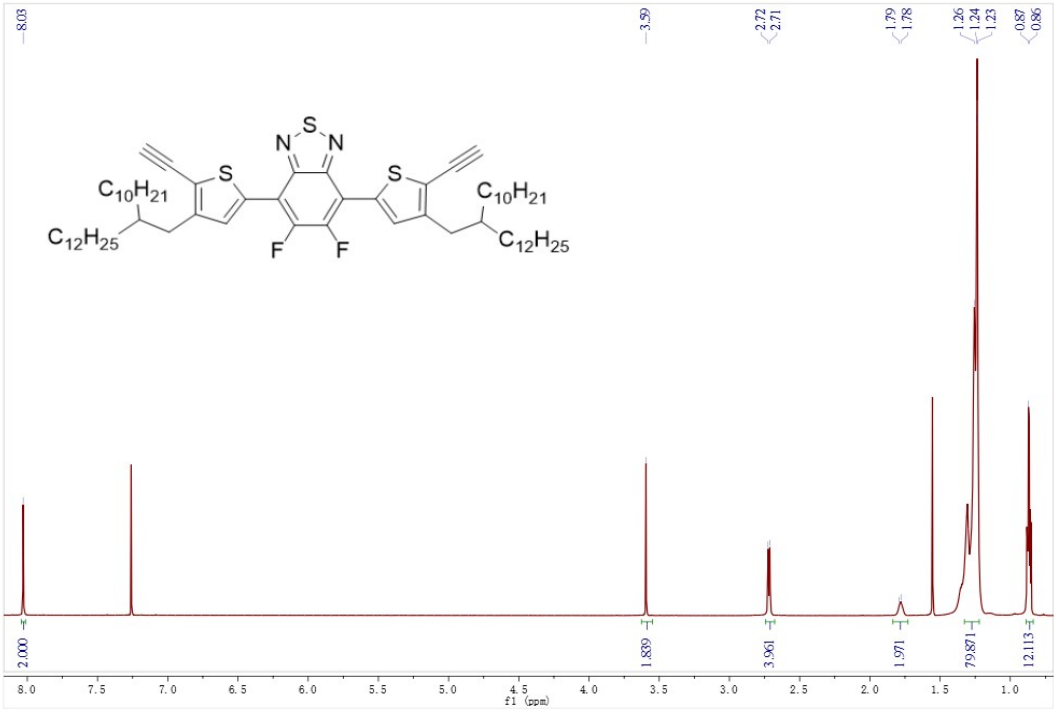

^{1}H NMR (400 MHz, Chloroform-*d*) of **Monomer ffBT-2ET-2DT**: δ 7.87 (s, 2H), 7.81 (s, 2H), 3.56 (s, 2H), 2.70 (d, *J* = 7.0 Hz, 4H), 1.79 (d, *J* = 8.4 Hz, 2H), 1.25 (d, *J* = 8.2 Hz, 80H), 0.87 (q, *J* = 4.0 Hz, 12H).

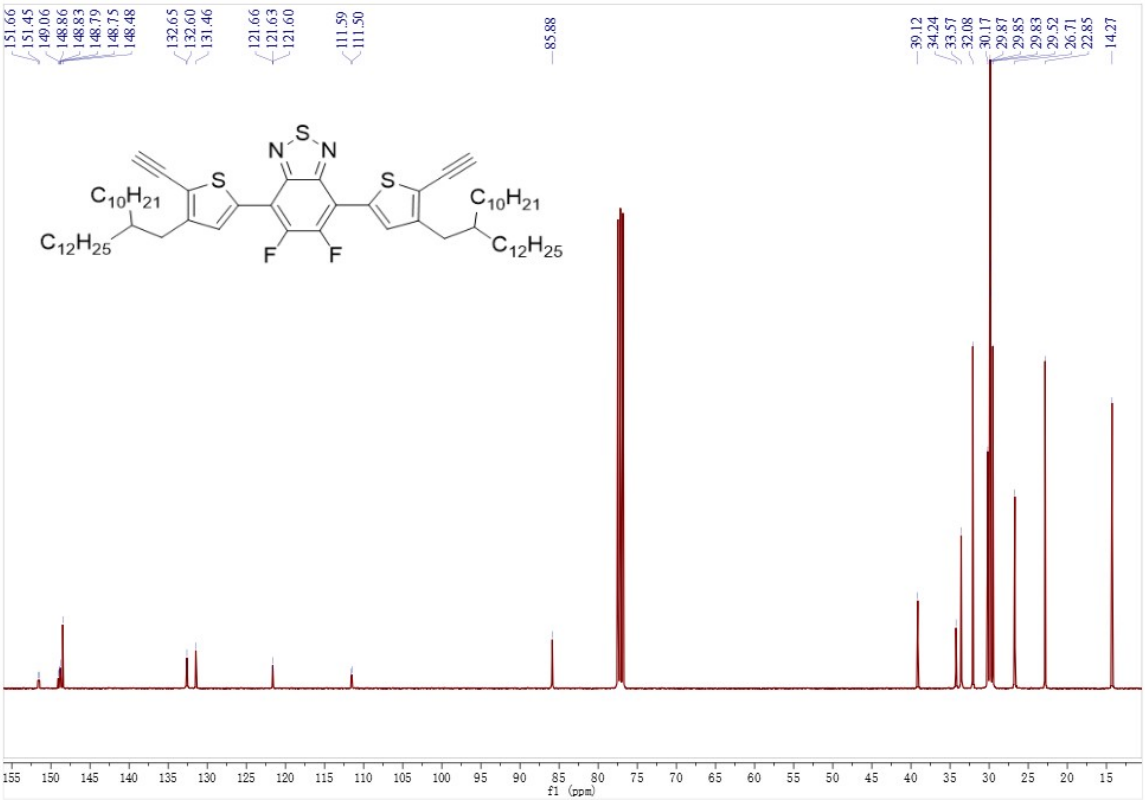

^{13}C NMR (101 MHz, Chloroform-*d*) of **Monomer ffBT-2ET-2DT**: δ 149.31, 129.21, 125.80, 125.73, 85.09, 39.13, 34.44, 33.59, 32.08, 30.18, 29.87, 29.85, 29.82, 29.52, 26.71, 22.84, 14.27.

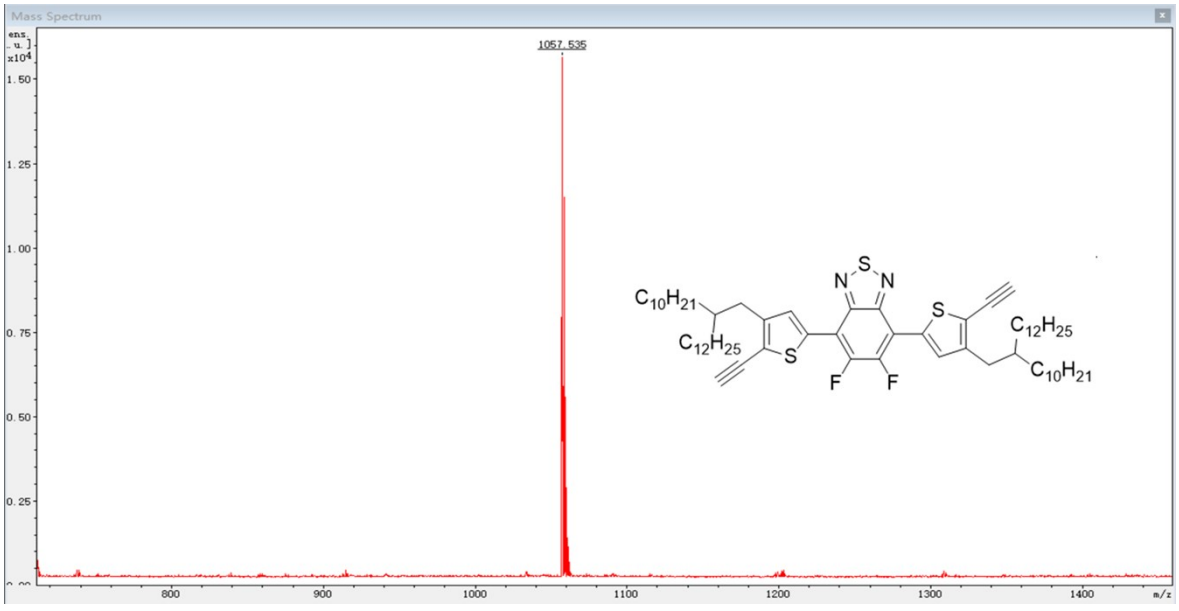

MALDI-ToF MS m/z: $[M+H]^+$ calcd. for $C_{66}H_{102}F_2N_2S_3$, 1056.72; found, 1057.535.

References

1 C. Chen, Y. Li, J. Song, Z. Yang, Y. Kuang, E. Hitz, C. Jia, A. Gong, F. Jiang, J. Y. Zhu, B. Yang, J. Xie and L. Hu, *Advanced Materials*, 2017, **29**, 1701756.

2 Y. Kuang, C. Chen, S. He, E. M. Hitz, Y. Wang, W. Gan, R. Mi and L. Hu, *Advanced Materials*, 2019, **31**, 1-8.

3 X. Wu, M. E. Robson, J. L. Phelps, J. S. Tan, B. Shao, G. Owens and H. Xu, *Nano Energy*, 2019, **56**, 708-715.

4 Y. Lu, D. Fan, Y. Wang, H. Xu, C. Lu and X. Yang, *ACS Nano*, 2021, **15**, 10366-10376.

5 M. N. A. S. Ivan, S. Saha, A. M. Saleque, S. Ahmed, A. K. Thakur, G. Bai, Z. Miao, R. Saidur and Y. H. Tsang, *Nano Energy*, 2024, 120, 109176.

6 Y. Yuan, C. Dong, J. Gu, Q. Liu, J. Xu, C. Zhou, G. Song, W. Chen, L. Yao and D. Zhang, *Advanced Materials*, 2020, **32**, 1907975.